*Pure & Appl. Chem.*, Vol.53, pp.421-448. 0033-4545/81/0201-0421$02.00/0
Pergamon Press Ltd. 1981. Printed in Great Britain.
©IUPAC

# PHASE STRUCTURE OF POLYVINYL CHLORIDE (PVC) AND PVC/POLYMER BLENDS

Björn Terselius and Bengt Rånby

Department of Polymer Technology, The Royal Institute of Technology, Stockholm, Sweden

Abstract - Commercial PVC is considered as a largely amorphous glassy polymer containing a small fraction of crystalline (ordered) structure. Based on the unique strength of plasticized PVC the presence of a three dimensional network of crystallites is generally accepted. The crystallites consist of a small number of syndiotactically ordered monomer units. The exact size, order and amount of crystallites in PVC is still an open question. The morphology of "as polymerized" PVC is characterized by free-flowing grains (about 100 μm) containing aggregates of primary particles (about 1 μm). The existence of subprimary particles are often claimed but the evidence is still controversial. A remaining microheterogeneity after plasticizing with diallylphtalate or ethylene-vinylacetate copolymer with 63 wt-% vinylacetate is, however, indicating the presence of unplasticized nodules or crystallites.

The phase structure of PVC blends with acrylo-nitrile-butadiene rubber (NBR), ethylene-vinylacetate copolymer (EVA) and chlorinated polyethylene (CPE) have been elucidated with special reference to the formation of a network structure. The phase structure is shown to depend on compatibility, method of blending and processing temperature at mechanical blending. Thus at increasing compatibility i.e. by increasing the content of acrylonitrile, vinylacetate and chlorine in NBR, EVA and CPE, respectively, the phase inversion of PVC to rubber as continuous phase, is shifted from about 15 to about 2% content of rubber. Increasing the mechanical processing temperature from below to above the critical temperature of primary particle fusion shifts the phase inversion to higher rubber contents (about 30% for non-compatible rubber). At solution blending the inversion is shifted to still higher rubber contents (about 50%). The phase structure of blends with ABS-type of polymers are briefly reported and the possibility of network structure formation is discussed. Finally, blends with crystallizable polymers like polycaprolactone (PCL) and Hytrel (a thermoplastic poyester-ether rubber) are reviewed. The amorphous segments of these polymers are compatible with PVC.

## PHASE STRUCTURE OF PVC

### Introduction

PVC has been produced and processed in large volumes for a long time on account of its versatile properties in relation to its low price. Nevertheless, the polymer is still considered "difficult" and its basic properties to a large extent unexplored (1). These problems can be discussed in terms of structure on a molecular,intermolecular and supermolecular level.

Thus the molecular weight and the molecular structure are difficult to vary and characterize. Thermal degradation of the polymer follows pathways which are not well understood and cause experimental problems in measurements of changes occuring especially at high temperatures. During processing of PVC the risk of thermal degradation and oxidation together with high melt viscosity presents a very unfavorable combination. Also the polymerization of PVC presents problems by requiring special equipment and handling procedures. In addition the polymerization kinetics is complex.

On an intermolecular scale we find the degree and nature of crystallinity in PVC to have been a matter of great controversy. The fact that the polymer is neither completely amorphous nor highly crystalline makes it difficult to find comparable data for other polymeric materials for the interpretation of data. Recrystallization at temperatures above Tg makes control of the termal history important.

On a supermolecular level the fusion or gelation of the primary particles of PVC during pro-

cessing still have not been given a satisfactory interpretation. There is no simple way of monitoring gelation levels. This important process in the manufacture of extruded rigid PVC products is yet to be described in basic terms.

Chain branching of PVC

The total amount of chain branching in PVC has generally been evaluated by reduction of PVC to polyethylene using lithium aluminium hydride, followed by determination of the content of methyl groups by IR spectroscopy and lately by $^{13}$C-NMR.

It has been accepted since the 1950:ies that short chain branching predominates in PVC. However the number of branches has been a controversial matter.

Cotman (2) first determined the number to 7 branches per 1000 C-atoms in commercial PVC. Similar results were reported by Bier and Kramer (3). Some authors have reported 15 to 20 branches per 1000 C-atoms (4,5) while others found only 2 to 5 side chains per 1000 C-atoms in commercial PVC (6,7).

All these IR investigations were based upon the assumption that the side chains were of butyl type (4 C-atoms). It was later shown by Rigo et al (8) that the side chains were instead methyl groups. Abbås (9,10) conclusively established by $^{13}$C-NMR that the side chains were pendant chloromethyl groups.

Since the IR extinction coefficients for methyl and butyl side chains were shown to be different (11) Abbås (9,12,13) and Park (14) concluded that the number of short side chains as determined by IR-measurements were overestimated by a factor of about two.
By $^{13}$C-NMR Abbås (9,10) determined the number of short side chains to 3 per 1000 C-atoms and of long side chains to about 1 per 1000 C-atoms, largely independent of polymerization temperature in the range 40 to 75$^{o}$C.

By decreasing the polymerization temperature branching is reduced (6) and at -50$^{o}$C PVC is considered as essentially linear (7,8,15) although a certain degree of branching has been reported by some authors (4,16).

Tacticity

In commercial PVC a tactic structure is dominating. However, as discovered by Natta and Corradini in 1956 (17), short sequences of syndiotactic structures also exist. By IR and NMR spectroscopy several authors (6,18-21) have shown that by decreasing the polymerization temperature the syndiotacticity of PVC is increased (see Fig. 1). It has also been shown (23) that decreasing the polymerization temperature increases the weight fraction of longer syndiotactic sequences (see Fig. 2).

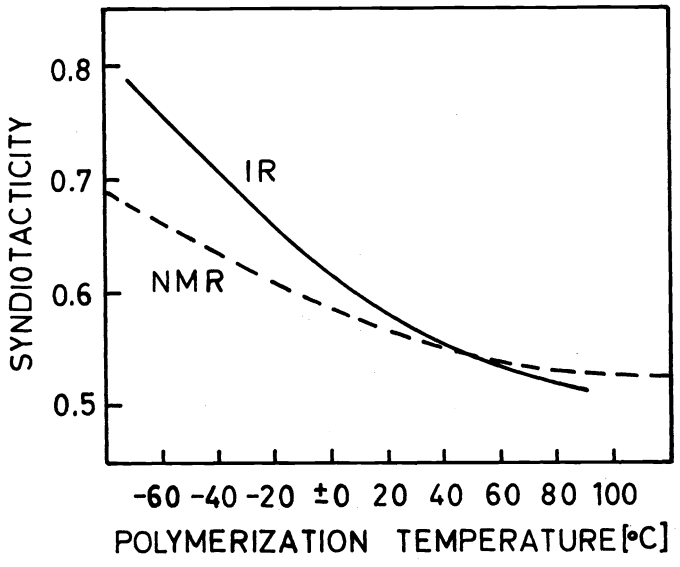


Fig.1. Syndiotacticity (1-σ) of PVC obtained from IR measurements (Germar, Nakajima) and NMR measurements (Talamini, Bovey, Cavalli) vs. polymerization temperature; from Pezzin (22).

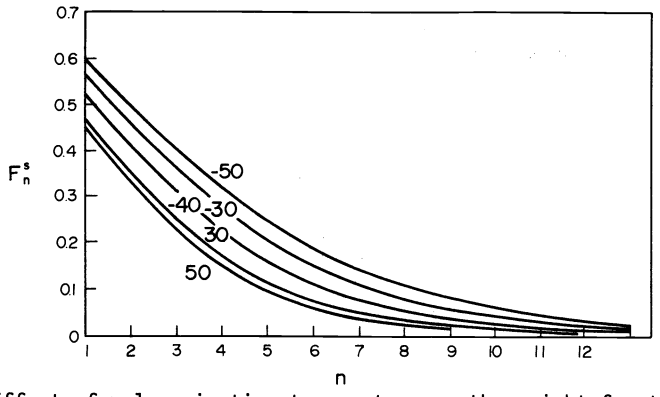


Fig.2. Effect of polymerization temperature on the weight fraction of syndiotactic sequences ($F_n^s$) of length greater than n monomer units; ref. (23).

## Crystallinity

Introduction. Commercial PVC is considered as a largely amorphous glassy polymer containing a small fraction of crystalline structure. Creep tests by Leaderman (24) and relaxation studies by Tobolsky et al (25) long ago suggested crystallinity to be the cause of the unique strength of plasticized PVC. Tobolsky et al (25) also postulated a model of a three-dimensional network of crystallites to explain the mechanical behaviour of the material. Later this theory has been supported by Pezzin and Berens (26), Münstedt (27,28) and Manson (29,32)

Crystal structure. Early X-ray investigations by Natta and Corradini (17) of oriented fibers

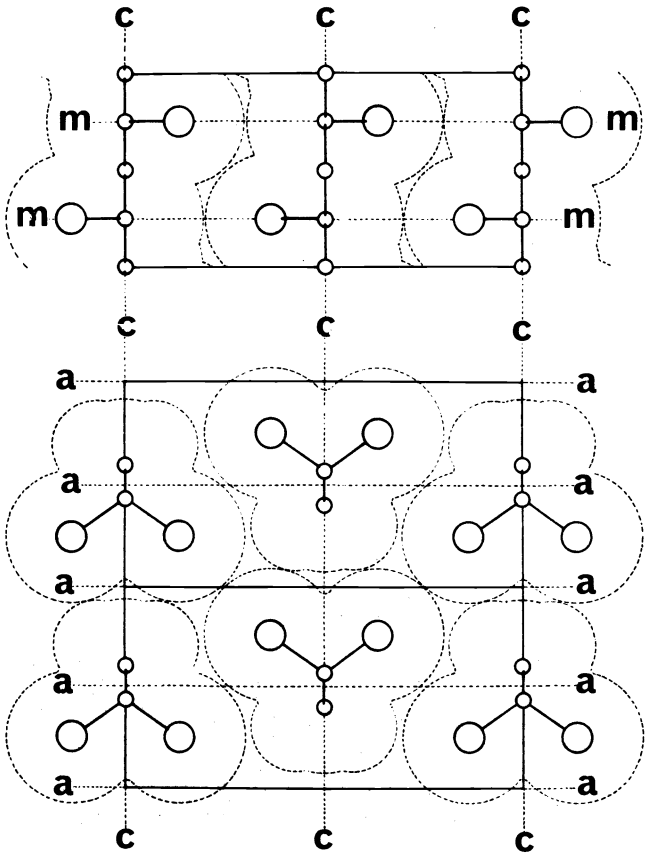


Fig.3. Model of the structure of PVC with syndiotactic straight chains in an orthorombic lattice, ref. (17).

of low crystalline syndiotactic PVC showed the presence of an orthorombic unit cell the approximate dimensions of which were given. Later Wilkes et al (28) made a more accurate determination of the unit cell dimensions (a = 10.24 Å, b = 5.24 Å, c = 5.08 Å) from X-ray diffractograms of oriented single crystals of PVC (see Fig.3). The crystal density was calculated to be 1.53 g/cm$^3$.

Crystallites. From wide angle X-ray scattering (WAXS) diagrams Natta and Corradini concluded the existence of laterally ordered domains, about 5 nm wide and quite short along the chain axis. Similar crystallite sizes (5 to 10 nm) have been reported by several authors (29-34) on the basis of X-ray diffraction studies. Values below 5 nm have occurred in the literature (35). D'Amato and Strella (19) estimated the crystallite size to the order of 1 nm from WAXS measurements.

More detailed descriptions of the crystallites have also been given. Thus Manson et al (32) consider the chains arranged in a manner similar to the fringed micelle model with thin (10--15 Å) lamellar crystallites 5 to 10 nm wide connected by rather long disordered chain segments. Wenig (33) interpreted his WAXS, SAXS and small angle light scattering (SALS) data in terms of lamellar crystallites forming "domains" or "subprimary particles" of 23 nm (see Fig. 4).

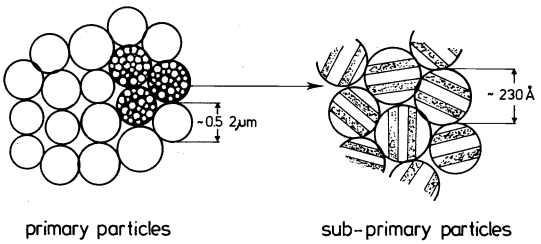


Fig. 4. Model of internal structure organization of PVC grains.Wenig(33).

Some authors report SAXS-intensities monotonically decreasing with increasing scattering angle: Nielsen and Jabarin (34) interprete their data in terms of a bimodal distribution of scattering elements around 6 and 50 nm. Considering that no slit smearing correction was undertaken these figures seem uncertain. Geil et al (37) do not draw any conclusions from their SAXS curve for unplasticized PVC (see Fig. 5 ) while Straff and Uhlmann (38) attribute

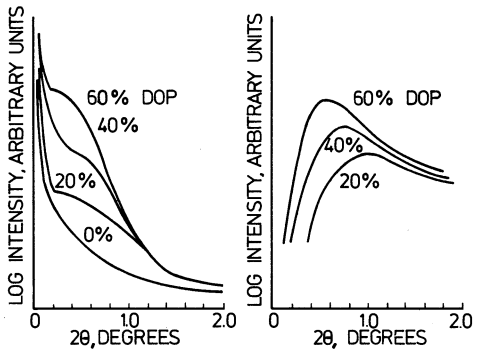


Fig. 5. SAXS scans of PVC/DOP blends a) uncorrected b) corrected for background sample absorption, etc; ref. (37).

the high scattering intensities at low angles to heterogeneities up to 450 nm and the low intensities at high angles to heterogeneities down to 5 nm and to thermal fluctuations.

Crystallinity. For conventional almost atactic PVC several authors have estimated the crystallinity by WAXS or by differential scanning calorimetry (DSC) measurements to 5% or less (35,39,40). Most authors estimate the crystallinity to 5-10% (18,31,33,36,41). From density measurements Nakajima et al (6) obtain a value of 12% while Straff and Uhlman (38) based on SAXS data suggest a crystallinity of less than 0.5 vol.%.

Length of ordered monomer sequences. The order along the chain axis is poor (17,42). The length or thickness of the crystallites have been estimated to a sequence of between 5 (18,

43) and 12 (44) predominantly syndiotactically ordered monomer units.

According to Juijn et al (42) a maximum crystallinity of 0.45% is obtained from statistical sequence length distributions when the minimum sequence length for crystallization is set to 12 monomer units and the syndiotacticity is assumed to be 0.55. A crystallinity of 5-10% would correspond to a minimum sequence length of 6-7 monomer units. Juijn postulates incorporation of isotactic straight chains into the orthorombic crystals to account for the improbably short minimum sequence lengths of syndiotactic units.Some authors (18,45) estimate the minimum number to be 5 units, which is consistent with the poor order along the chain axis.

Polymerization temperature. Crystallinity in PVC increases with decreasing polymerization temperature primarily as a consequence of increasing syndiotacticity and to some extent due to decreased chain branching. For PVC prepared at -50°C crystallinities of 20% have been reported (18,31,35,46). At -60°C 25% (47) and at -75°C 27% crystallinity (32) have been obtained. Nakajima (6) reports values of crystallinity, generally three times as high based on density measurements.

## Supermolecular structure

Morphology-characterization terminology. At "The Second International Symposium on Polyvinylchloride, July 5-9, 1976, Lyon" a strict terminology for the characterization of the morphology of PVC proposed by Geil was accepted and strongly recommended for future use (see Table 1).

TABLE 1.

| Term | Approximate size in typical PVC | Origin or description |
|---|---|---|
| Grain | 100 μm | Free flowing at room temperature |
| Agglomerate | 10 μm | Formed during polymerization by merging of primary particles |
| Primary Particle | 1 μm | Formed from single polymerization site at conversions of 10-50% |
| Domain | 100 nm | Presence not clearly proven, possibly formed by mechanical working within or from primary particles |
| Microdomains | 10 nm | Crystallite or nodule? |

Morphology of "as polymerized" PVC. PVC is commercially polymerized in mass, suspension or emulsion. From the polymerization process primary particles are obtained clustered and to some extent fused together to form grains of varying porosity. The orders of size for these particles is seen in table 2 and their general morphology is evident from Fig.6. Suspension grains generally differ from mass grains in being covered by a skin or according to Tregan (51) a "pericellular membrane" about 0.5 μm thick although skin-free S-PVC can be produced, for example PEVIKON S-688 from KEMANORD AB, Sundsvall, Sweden. Mass grains retain their agglomerated particle structure from the interior out to the surface, which is rounded and slightly compacted. Both types of grains contain small interstitial voids. S-PVC also has larger skin-covered voids.

TABLE 2

| | Primary Particles size (μm) | Grains size (μm) |
|---|---|---|
| M-PVC | 0.5 - 1.5 | 50 - 100 |
| S-PVC | 0.5 - 1.5 | 75 - 250 |
| E-PVC | 0.15- 0.40 | 50 - 150 |

Emulsion grains vary in size with the latex-drying conditions. They consist of small spheri-

cal, loosely agglomerated primary particles. The general morphology of these grains is a consequence of the insolubility of PVC in its monomer.

The nucleation and growth of primary particles are common to S- and M-PVC. In fact suspension polymerization within a monomer droplet can be looked upon as a micro mass polymerization. The process has been described by many authors (48-57) and is schematically illustrated by Barclay (48), see figure 7, Shinagava (49), see figure 8, and Hattori (57), see figure 9. As soon as initiator contacts monomer, nascent particles of about 10 nm size consisting of a few coiled macromolecules are precipitated from the monomer phase. At less than 0.1% conversion the nascent particles aggregate to form embryonal primary particles of up to 0.1 μm size. These possess colloidal stability due to surface adsorption of chloride ions, the origin of which is unclear (56). The embryos grow by capture of macroradicals from the VC phase (54). At less than 1% conversion the growing primary particles flocculate and growth proceeds in the flocs until micron size is reached.

Characterization techniques for the large scale superstructure of PVC-grains. The large variety of spatial arrangements of primary particles within grains results in a broad spectrum of internal grain porosities. The most common test methods used to describe the porosity are the mercury intrusion porosimetry (58), permitting intruded volumes and average pore sizes to be calculated, and the standard nitrogen adsorption method (BTE) for specific area determination. Other methods are based on estimation of bulk density, plasticizer absorption and dry-up times. These methods give average data on porosity. Estimations of porosity distribution can be gained (59) by observing density distribution of PVC-grains by sedimentation in wetting but not swelling solvent mixtures. Following the adsorption of DDP or silicone oil by the grains with optical microscopy. Examination of fracture surfaces of grains embedded in wetting but not swelling media like epoxi resin by SEM also gives information of the distribution of porosity (59). The interior of grains can also be exposed by cutting with a scalpel or with a glassknife in an ultramicrotome and subsequent observation in SEM. Some attempts to find structures inside primary particles will be reviewed. Thus Cobbold and Mendelson (75) in 1971 published a transmission electron micrograph of freeze sectioned PVC grains embedded in a fast curing polymethylmethacrylate resin (see Fig 10). It is well-known that methylmethacrylate swells PVC to a considerable extent and that PMMA is compatible with PVC. As a result by a normal embedding in MMA which is polymerized, a kind of "exploded view" of PVC is obtained. The contrast is excellent on account of the low radiation resistance of PMMA and resulting mass loss when irradiated. Use of a fast curing PMMA imposes a rather mild swelling action on the PVC-particles. The authors present the micrograph as proof for "existence of particle substructure" but admit that "detailed interpretation of the contrast effects is obscure" on the grounds presented above. In fact we believe that every interpretation of a micrograph of a MMA embedded PVC sample is a most hazardous adventure. Hattori (57) also used the MMA embedding method and reported that it "clearly reveals a detailed structure of the inside grain" (see Fig. 11). Epoxy embedding on the other hand did not swell the structure and thus no substructure was exposed.

From SEM pictures at rather high magnification of PVC-grains, embedded in epoxi resin and freeze-fractured, Krzewki and Sieglaff (59) claim to have detected submicroparticles (domaines) of 40 to 80 nm inside primary particles (see Fig. 12).

Although a considerable support exists for the idea of primary particles being formed by agglomeration of domaines, conclusive evidence of the existence of domains after polymerization is still lacking.

Melt flow units. Melt flow behaviour is generally interpreted in terms of molecular structure parameters such as molecular weight, molecular weight distribution, chain branching etc., and not so frequently in terms of supermolecular structure. Supermolecular flow units were first postulated by Mooney (61). Berens and Folt (62) were the first to correlate the reduction in melt viscosity at lower flow temperatures for PVC with the presence of a particulate structure as shown by fracture surface micrographs. The topic has been extensively reviewed by Collins (63). Collins and Krier (64) reported that the melt flow of E-PVC showed two different flow activation energies in the range of 160° to 230°C at a series of shear rates (see Fig. 13). This dual flow mechanism was also found for S-PVC (65) and was interpreted in terms of particular and molecular flow at lower and higher temperatures, respectively. The transition temperature was shifted to higher temperatures at higher shear rates. According to Berens and Folt (66) particle flow was favoured by decreased temperature and increased shear rate as well as by increased molecular weight, particle size and crystallinity.

For PVC plasticized with 50 phr DOP similar melt flow data as for pure PVC has been obtained but the transition temperature was lower, 165-170°C (37).

Some controversy concerning the nature of the flow units exists. Thus changes in melt flow

Fig.6

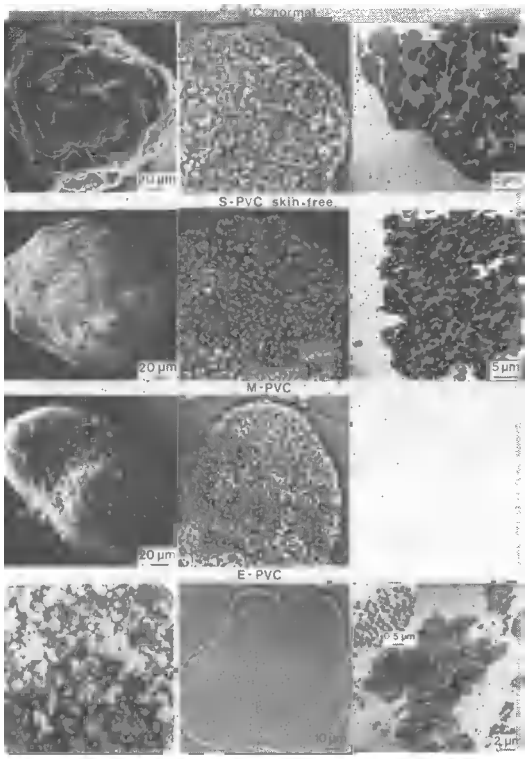


Fig.7

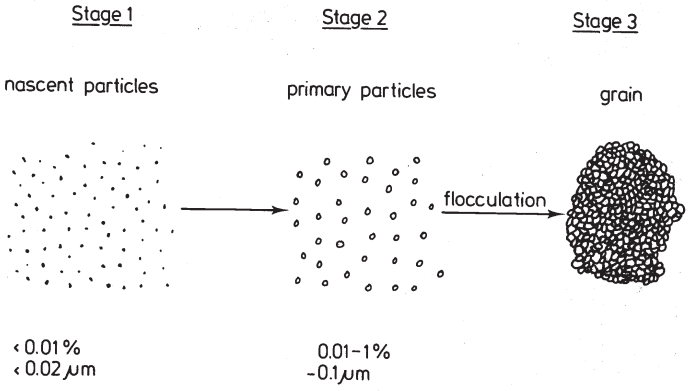


Fig.8

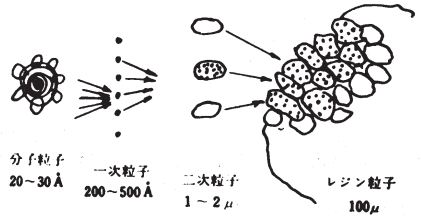


Fig.6. General morphology of PVC grains from suspension, mass and emulsion polymerization, elucidated by SEM, OM and TEM(courtesy of KEMANORD AB).

Fig.7. Schematical illustration of growth of suspension and mass polymerized PVC particles; ref.(48).

Fig.8. Formation of PVC grain; ref.(49).

Fig.9

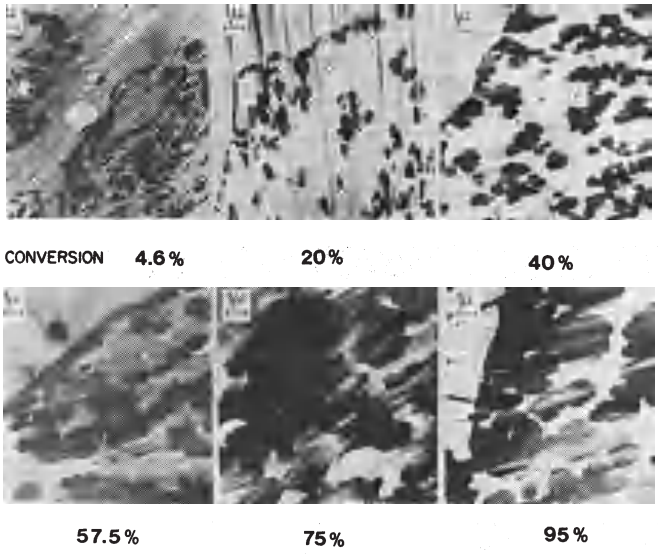


Fig.10

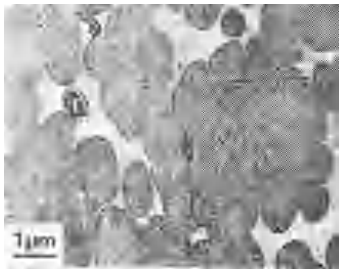


Fig.11

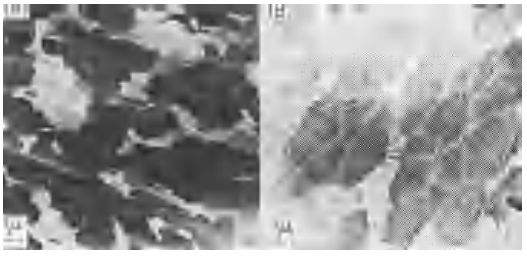

Fig.12

Fig.13

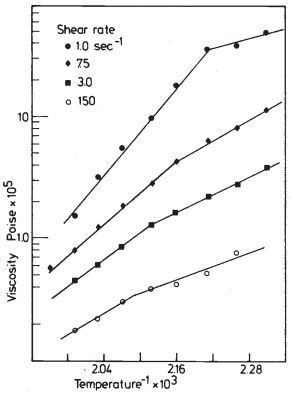


Fig.9. Change of morphology of PVC grains during the polymerization process. The grains were embedded in epoxy, sectioned and observed in TEM. At 4.6% conversion the particle size is about 0.1 µm. Full size, 1 µm, is reached at 40% conversion; ref.(57).

Fig.10. Morphology of PVC grain, embedded in methylmethacrylate (MMA) showing artefact structure inside the primary particles; ref.(75).

Fig.11. Morphology of PVC grain, embedded in (A) epoxy (B) MMA; ref.(57).

Fig.12. SEM picture of fractured primary particle showing internal structure; ref.(59).

Fig.13. Arrhenius plot showing dual activation energy for PVC-flow;ref.(64).

behaviour has been explained in terms of crystallinity (67-69) and reversible structural changes in a network of crystallites (68,69), as well as in terms of an irreversible particle fusion (65). Berens and Folt (62) regard the particles as entities held together by a network of entanglements.

The system may be looked upon in the following way. With respect to the shear field and temperature an equilibrium number of stable crystallites and/or entanglements exists. Decreasing the temperature or increasing the shear forces imposes a reversible increase of the number of stable crystallites and/or entanglements, thereby stabilizing the particular structure. On the other hand melting of crystallites and disentanglement are accompanied by interparticle diffusion of segments and particle fusion as well as by formation of new particles with size and stability determined by the shearing and thermal conditions rather than by the polymerization history.

Morphology of processed PVC. At processing of PVC powder by heat and shear, generally between 160 and 190°C, the grains are first broken down to primary particles acting as flow units. At about 190°C the primary particles are fused and broken down to smaller flow units the identity of which is not very clear. It is well known that heat alone is hardly sufficient to fuse primary particles (57,70,71). PVC-powder kept as 220°C for 1 minute still contained primary particles (57).

Faulkner (72) describes a technique for determination of a "Temperature - torque Profile for PVC-compounds in a Brabender Plastograph". Three characteristic peaks are obtained. From observations by TEM of carbon replicas of ion-beam etched surfaces and by SEM these peaks are attributed to break-down of grains, primary particles and most hypothetically of microdomains, respectively (see Fig. 15-A).

Thus the large-scale superstructure of processed PVC is rather well known. However, the small scale structure and its relation to process history is still much of an open question.

Perhaps the most quoted investigation of the morphology of processed PVC is the one by Hattori (57). In 1972 Hattori published transmission electron micrographs of PVC extruded at exit temperatures ranging from 160 to 210°C, embedded in MMA and ultrasectioned (see Fig. 14).

The primary particle structure is preserved up to 180°C, where it is broken down into a more or less continuous network which in turn at 190 to 200°C is broken down to fibrils. These fibrils are of the order of 30 nm and may be swelled 100 to 200% but not destroyed by the MMA action. Based upon these observations as well as observations of similar fibrils in MMA swollen primary particles of not processed PVC, the authors assume that the fibrillar structure exists in the primary particles of PVC as polymerized and propose the following structure organization (see Fig. 15-B).

The primary particles are supposed to be built up by a network of fibrils. The authors link this model together with the classical concept of a crystallite network as the framework in plasticized PVC.

The microheterogeneity still left in plasticized PVC is also illustrated in the publication of Hattori by an electron micrograph of PVC plasticized with 45% by weight of diallylphatalate (DAP). DAP was selectively stained by osmiumteteroxide ($OsO_4$) and occurred as dark DAP-rich microdomains of the order of 10 nm, but occasionally up to 0.2 μm, dispersed in a bright PVC-rich matrix (see Fig. 16).

A similar study of the phase structure of PVC plasticized with 33% by weight of tetraethyleneglycol dimethacrylate (TEGDMA) was performed by Bair et al (73). The TEGDMA-rich phase was selectively stained by $OsO_4$. The phase structure was rather complex with primary particles containing a fine dispersion of TEGDMA-rich microdomains and an interparticle phase containing finely dispersed PVC-rich microdomains (see Fig. 17).

Dynamic Mechanical Spectroscopy (DMS) and Differential Scanning Calorimetry (DSC) showed the presence of two transitions at about -60 and -25°C attributed to the TEGDMA-rich and PVC-rich microphases, respectively. The transitions were not changed by harder processing with fusion of the primary particles indicating that the transitions actually originate from co-operative segmental motion inside the microphases.

Bonart (74) interpretes the plasticizer action in PVC from electron micrographs and SAXS data in terms of swelling of interlamellar regions.

Geil et al (37) on the other hand find no lamellae in plasticized PVC. From transmission electron micrographs of platinum - carbon replica of freeze - fracture surfaces of S-PVC plasticized with 10 to 60% by weight of dioctylphtalate (DOP), Geil and his coworkers in-

Fig.14

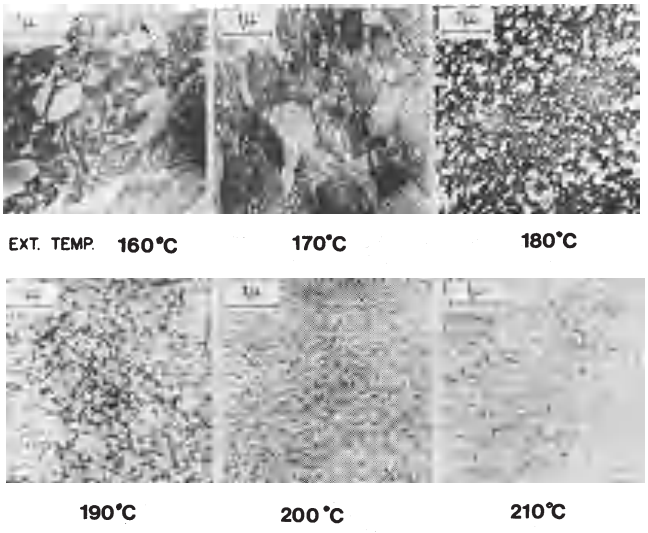


Fig.15

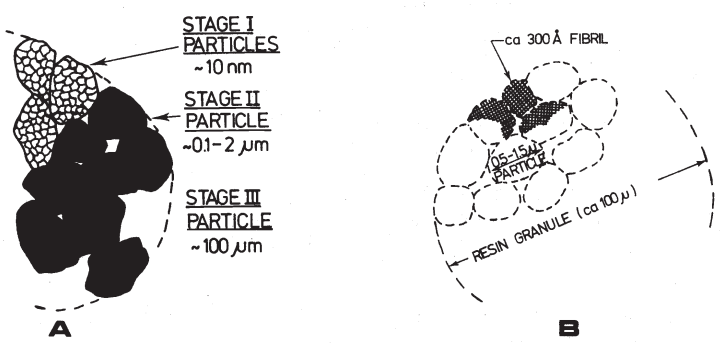


Fig.16

Fig.17

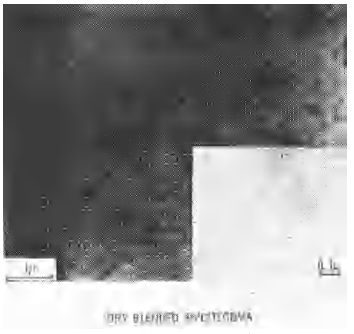

Fig.18

Fig.14. Morphology of PVC extruded at different temperatures and embedded in MMA; ref.(57).

Fig.15. Different models of internal structure organization of PVC grains. (A) Faulkner(72), from Hori(76), (B) Hattori(57), see also Fig.4.

Fig.16. Electron micrograph of PVC/Diallylphtalate (DAP) blend, (55/45) showing fine dispersion of DAP-rich phase (stained by $OsO_4$) in PVC-rich matrix; ref.(57).

Fig.17. Electron micrograph of PVC/TEGDMA blend (77/33) showing fine dispersion of TEGDMA-rich microdomains in PVC particles and interparticle phase containing finely dispersed PVC-rich microdomains; ref.(73).

Fig.18. Electron micrograph of freeze-fracture surface of PVC/DOP blend (40/60), showing nodules of 20 nm and domains of 0.1-0.2 nm; ref.(37).

stead found nodules of 10 to 20 nm increasing in size with plasticizer content. These findings agreed well with SAXS data on these materials (see Fig. 18 and Fig. 5). The nodules varied in visibility and distinctness with processing conditions probably because of incomplete plastication. Also 0.1 μm domains were found. No correlation between the nodules and the crystallites presumably present in plasticized PVC could be established. In fracture surfaces of unplasticized PVC the authors are very uncertain about the existence of nodules. Ion-etching of the fracture surfaces by high frequency generated ionized air or argon (71) increases small scale structure of the surfaces but on account of local heating and unclear mechanism, interpretation seems hazardous. SAXS curves for unplasticized PVC showed no maxima (see Fig. 5).

## PVC-BLENDS

### Introduction

In order to increase the processability and ductility of PVC, polymer modifiers are often added. As processing aids polyacrylates and methacrylates (acrylics), styrene-acrylonitrile (SAN) and styrene-methacrylate copolymers have been used (1). The acrylics which appear to have been the most popular processors increase the fusion rate without affecting melt viscosity. Their compatibility with PVC is considerable although no plasticizer action is reported (1). Unlike the processors, impact modifiers only show limited compatibility with PVC. The reason for this is the criteria for increase of impact strength by a modifier as expressed in the classical work of Mertz, Claver and Baer (2) stating that the impact modifier should

- form a second phase
- have a low $T_g$
- show good phase adhesion
- be crosslinked

Since these authors were concerned with high impact polystyrene (HI-PS) and ABS they considered the second phase to be dispersed crosslinked rubber particles only. However, in PVC the impact modifier may just as well form an uncrosslinked continuous network structure. Thus when nitrile-butadiene rubber with 20% acrylonitrile (NBR-20), ethylene-vinylacetate copolymer with 45% vinylacetate (EVA-45) or chlorinated polyethylene with 36% chlorine (CPE-36) is blended with PVC the impact resistant two-phase system must be produced by mechanical processing of the mixture. Experience has shown that moderate processing breaks down the original PVC-grains to primary particles but does not fuse them. If a rubbery material like NBR-20, EVA-45 or CPE-36 is moderately processed together with PVC in a concentration of at least 5-6%, it will form a continuous rubbery network embedding the primary particles (3-5). This network may increase the impact strength of PVC by up to 25 times (1). If the mixture is processed harder with respect to temperature, time or shear field, fusing of the primary PVC particles will be brought about and the network will be broken down into small irregular rubber particles. By this change of structure (phase inversion) the impact resistance will be totally lost (5-7), (see Fig. 19 and Fig. 20).

High impact and transparent PVC blends may be obtained by adding modifiers already containing small and well defined rubber particles such as ABS or MBS copolymers. In addition to transparency these modifiers exhibit a lower $T_g$ of the rubbery phase, i.e. a better low temperature impact strength. The disadvantage is reduced thermal and UV-stability due to the unsaturated rubber structure. Acrylic grafts with PVC have been developed with excellent transparency, impact strength and outdoor weatherability containing small well defined saturated rubber particles with a low $T_g$ (8).

### Acrylonitrile-Butadiene (NBR) Blends.

These copolymers exhibit in a certain composition range a compatibility with PVC that is quite unusual among polymers (9-13,21,22). Nielsen (9) first showed the existence of one single broad glass transition extending from the $T_g$ of pure NBR to that of pure PVC (see Fig. 20). Takayanagi (12) described these compatible polyblends as microheterogenous and applied a mechanical model to fit DMS-data. Horwath (14) found that PVC/NBR latex blends with two Tg's became more homogenous and showed only one broad glass transition after thermomechanical processing although TEM revealed a remaining microheterogeneity of up to the order of 0.1 μm.

In 1969 Matsuo et al (15) published transmission electron micrographs of mechanical blends of PVC and NBR processed at 155°C for 15 min. with six different acrylonitrile contents ranging from 0 to 40% (see Fig. 22 A-F) together with dynamic mechanical spectroscopy (DMS) data for some of these blends (see Fig. 23). Since these micrographs have generated several discussions on the morphology of not only PVC-blends but also on polymer blends in general we will give a detailed review of this investigation.

Fig.19

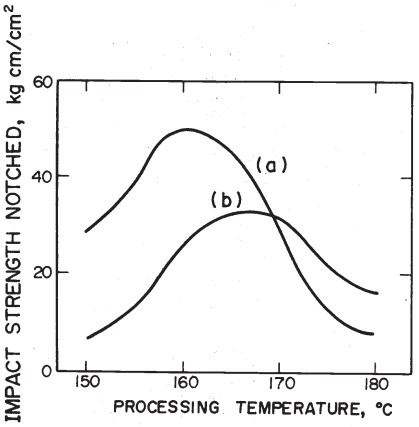


Fig.20

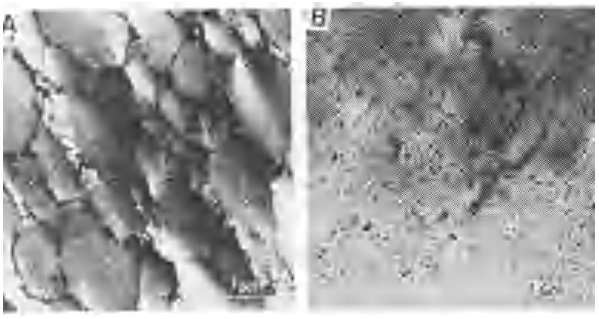


Fig.21

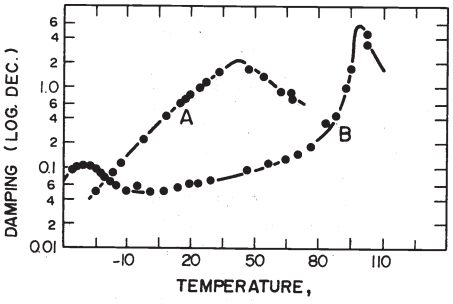


Fig.19. Influence of processing temperature on impact properties of vinyl-chloride/EVA graft copolymer (8% EVA); (a) PVC/EVA-45 (b) PVC/CPE-36; ref.(6)

Fig.20. Electron micrographs of PVC/EVA-45 blends, (94/6). A) Moderately processed showing rubber network, B) overprocessed showing rubber particles; ref.(4).

Fig.21. Dynamic mechanical loss tangent of polymer blends. a) PVC/NBR, b) PS/SBR; ref.(9).

Fig.22

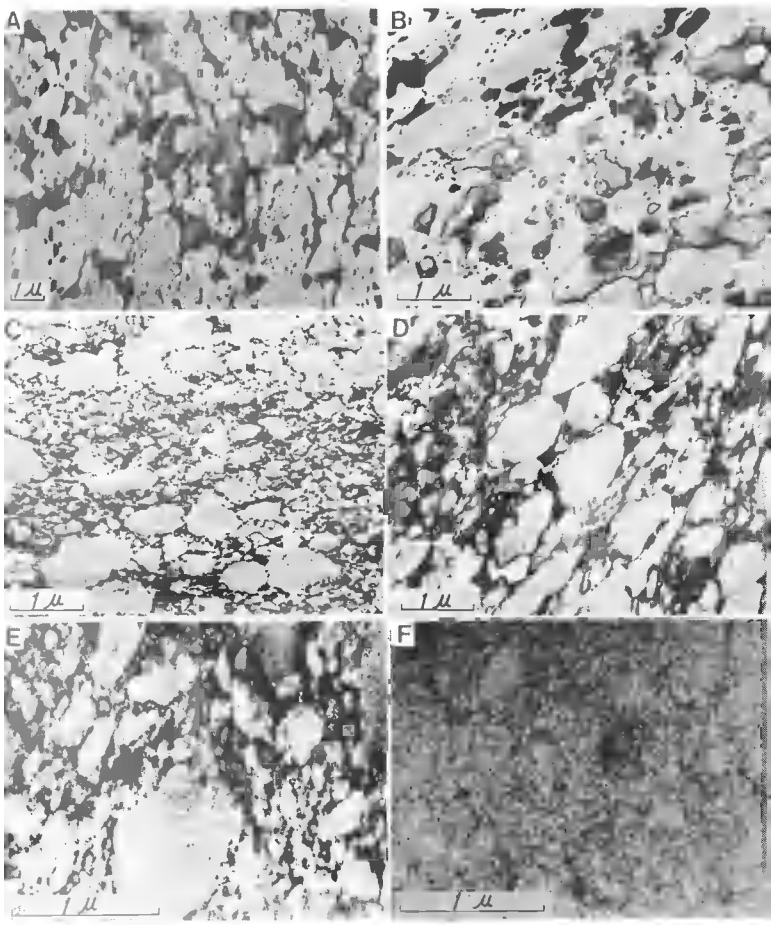


Fig.22. Transmission electron micrographs of PVC/NBR (100/15) blends with NBR of different AN contents. (A) 0%, (B) 8%, (C) 15%, (D) 20% (E) 30%, (F) 40%; from ref.(15).

Attempts to observe the original microstructure of ultrathin sections of PVC/rubber blends are rarely successful. The reason for this is that the structure needs fixation as well as higher phase contrast. The osmiumtetroxide ($OsO_4$) staining and hardening procedure developed by Kato (17) solved these problems in a one step process. The method is based on the selective reaction of $OsO_4$ with double bonds. The reaction can be carried out with $OsO_4$ as gas or dissolved in suitable solvents.

Polybutadiene is a nonpolar rubber which mechanically blended with PVC is coarsely dispersed as irregular rubber particles of varying sizes up to a few microns (see Fig. 22-A). If 8% AN is copolymerized with butadiene and dispersed in PVC the rubber particles become smaller. At 15% AN content the particles are much smaller and the increased polarity allows the rubber to wet the surface of the primary PVC particles, preventing them from aggregating. NBR-20 does not form particles but a fine network embedding the primary PVC particles. NBR-30 forms two types of structures, partly a network as in NBR-20 and partly microdomains of the order of 10 nm inside the primary particles. NBR-40 blends finally are completely microheterogenous containing rubber- and PVC-rich domains of the order of 10 nm.

Fig.23

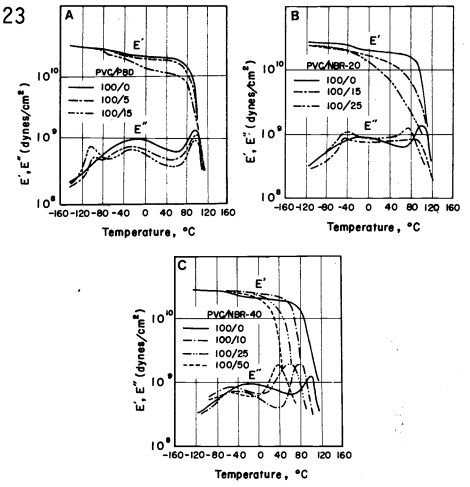


Fig.24

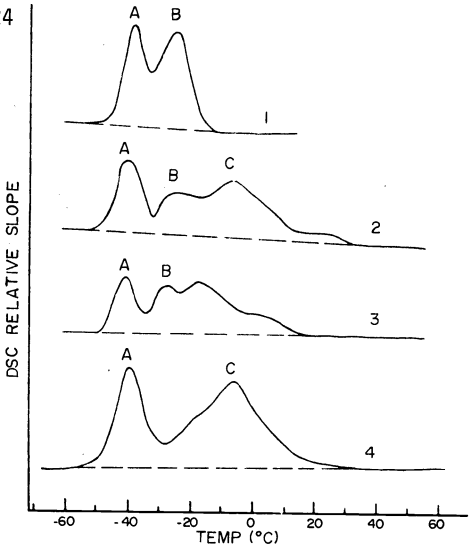


Fig.23. Dynamic mechanical spectrograms (DMS) forPVC/NBR blends of different compositions and different AN contents of NBR. (A) 0%, (B) 20%, (C) 40%; from ref.(15).

Fig 24. DSC slope curves of coflocculated PVC/NBR (30/70) blends containing two-phase NBR-29 (1) unprocessed, (2) heated in DSC to 170°C at 20°C/min and cooled at 80°C/min., (3) milled 3 min. at 177°C, (4) solution blend; ref.(18).

The PVC/PBD blends show two distinct glass transitions (see Fig. 23-A) at the temperature position of the pure components, respectively. NBR-20 blends with PVC have two transitions but the PVC transition is somewhat shifted indicating that the PVC phase is contaminated with rubber. PVC/NBR-40 blends show only one transition in an intermediate position between the transitions of the pure components shifting with blend proportions. Thus a strong molecular interaction is indicated in these blends.

High Contents of NBR. Landi (18) characterized the morphology of solution blended and mechanically processed PVC mixtures with NBR of different AN contents by DSC. NBR-34 blends showed one single transition temperature shifting with blend composition independent of method of preparation. NBR-29 blends, however, showed a complex transition pattern (see Fig. 24). The reason for this is that NBR with AN-content in the range of 25 to 30% is subjected to phase separation at high conversions of copolymerization (19.20). Thus two transitions were registred for NBR-29 corresponding to AN-contents of 23 and 30% respectively (20). Adding PVC to the NBR only affects the "NBR-30" transition broadening and shifting it to higher temperatures (see Fig. 24-4). This effect has also been reported by Jorgensen et al (21). Figure 24-3 indicates that the incompatible "NBR-23" phase (A) may act as a barrier for segmental interdiffusion of PVC and the compatible "NBR-30" phase (B) during milling. These findings may explain the bimodal size distribution of NBR-29 found by Matsuo et al (15) (see Fig. 22-E) as an incompatible "NBR-23" network and more or less compatible "NBR-30" microdomains inside the primary particles of PVC.

Landi (18) finds similarities in stress relaxation behaviour for PVC blends with liquid or solid NBR and DOP at 30 wt-% concentration. This leads him to assume the presence of a microcrystalline network similar to that widely accepted for plasticized PVC (34-36). This load-bearing PVC network should contribute to the excellent ozone resistance of vulcanized NBR/PVC by resisting growth of ozone cracks.

Low Contents of NBR. A further analogy between NBR and DOP is the ability of small amounts of NBR-42 to "antiplasticize" PVC. Bergman et al (27) found a minimum creep compliance and a maximum stress limit for linear viscoelasticity at 7 wt-% NBR-42. The effect is believed to originate from pseudocrosslinks between PVC chains blocking the coupling between $\alpha$- and $\beta$ -relaxation in PVC responsible for development of impact resistance as well as nonlinear viscoelasticity (28).

Ethylene-vinylacetate (EVA) Blends

EVA is a well studied modifier for PVC. As little as 5-8% of EVA of moderate VA-contents (around 45%) provides excellent impact strength, aging resistence and wheathering performance for outdoor applications. Higher VA-contents renders EVA a plasticizing effect on PVC. This is useful in flexible profiles or calendered flexible films etc., where migration of lowmolecular plasticiziers presents a problem. A disadvantage with EVA (as well as with CPE) blends with PVC is the mismatch of the refractive indicies of the components causing opaque products. For high impact purpose EVA-45 is used almost exclusively. The reason for this is obvious from Fig. 25. At 45 % VA the rubbery properties of EVA are optimized and so is the polarity with respect to the compatibility with PVC.

EVA-45. At the end of the sixties measurements at this laboratory of gas permeability (29,30) light scattering (31,32) and transmission electron microscopy (32) revealed to us the phase structure of mechanical blends and grafts of PVC/EVA-45.

The occurrence of a phase inversion at 4-7.5% EVA was indicated by a sudden increase in opacity. A marked increase in the optical heterogeneity parameter (31) and in the permeability

Fig.25

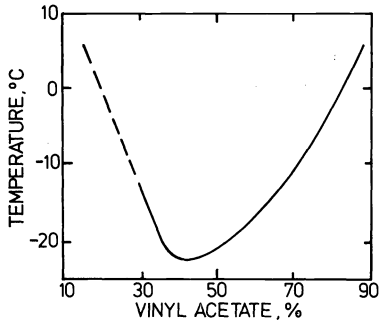


Fig.26

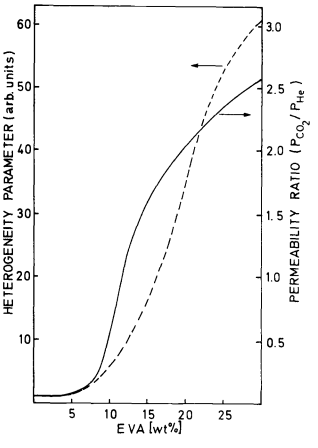


Fig. 25. Glass transition temperatures of EVA of different vinylacetate (VA) contents; ref.(6).

Fig.26. Heterogeneity parameter (from light scattering measurements) and permeability ratio for $CO_2$ and He vs composition, indicating phase inversion at 6-8 wt% EVA; from ref.(30,31).

ratio between $CO_2$ and He (30) (see Fig.26) supported this assumption. The inversion was confirmed by TEM showing rubber particles of the order of 0.05 µm at 4% EVA and the formation of a rubber network at 7.5% (see Fig.27).

The natural electron-optical phase contrast of ultrathin sections of PVC/EVA-45 is lost almost immediately at electron irradiation because of mass loss of the electron-dense PVC-phase. Therefore staining is necessary. The PVC-phase is very hard to stain but EVA can be made osmiofilic by alkaline hydrolysis of VA groups to VOH in refluxing methanol saturated with NaOH (33).

Svanson and Elmqvist (34) carried out wide line NMR measurements for protons on PVC/EVA-45 roll milled at 160°C for 15 min. They obtained a broad band, assigned to the PVC phase and a superimposed narrow band, assigned to the relatively mobile EVA phase. As the narrow band was less intense than expected the authors concluded that 2-3% EVA was dissolved in PVC. Annealing at 170°C for 40 min. increased the narrow band intensity to a level corresponding to phase separation except for blends with 2% EVA (see Fig.28) These were considered to form stable solutions.

In an attempt to verify these results DMS measurements were carried out on the same material with the same process history (35) As can be seen from Fig.29 no indication of molecular compatibility at low proportions of EVA can be detected. Annealing at 170°C for 1 hour did not change the temperature position or width of the EVA transition significantly. However, for samples with low EVA content (4 and 7.5% EVA) milled at 180°C there was a slight shift and/or broadening of the peaks. Annealing at 170°C for 1 hour tended to restore the original shape and temperature position of the peaks. These findings indicate a metastable phase structure in blends with low EVA content processed at 180°C but not at 160°C.

Solution blending of PVC/EVA-45 has been carried out by Marcincin et al (36) using 1% chlorobenzene solutions. DMS measurements showed a considerable shift of the PVC-peak towards the static EVA peak as EVA content is increased indicating that EVA is partially dissilved in PVC. Solution blends of PVC/EVA-45 from 2% THF solutions was shown by TEM to contain dispersed EVA of 0.5 µm size forming a continous phase at 30% content, see Fig.30 (39). The EVA phase showed a microgranular appearance indicating the presence of relatively EVA rich domains of 10 nm size in an EVA poor matrix.

Grafts of PVC/EVA-45. Grafts containing 7.5% EVA-45 in PVC are less opaque that the corresponding mechanical blends when processed at 160°C for 15 min. Light scattering measurements showed a clear decrease in the optical heterogeneity parameter (31,32). TEM revealed a considerably narrower PVC-particle size distribution with an average of 0.3 to 0.4 µm, i.e. somewhat lower values than for mechanical blends (see Fig.31).

The PVC particles are embedded in a well defined network with a string width of about 15 nm. The PVC particles seem to contain a 50 to 100 nm broad periferic zone showing radial tracks of EVA indicating a starting disintegration of the particles. Matsuo et al (37) have reported similar radially distributed EVA domains in PVC particles of grafts with 20% EVA-45 (see Fig.32). If the processing temperature of the grafts is increased to 180°C fusion of PVC particles breaks down part of the EVA network to particles of the order of 50 nm (see Fig.31B) DMS showed no effect of grafting on the peak position and width of the EVA phase in PVC/EVA (92.5/7.5) blends processed at 160°C. The effects of increasing the processing temperature to 180°C and of annealing at 170°C for 1 hour were the same as for mechanical blends.

The effect of grafting at higher EVA contents is a marked decrease in opacity and turbidity (29,30). Matsuo et al (37) showed that an increase of the EVA content from 5 to 50% in grafts of PVC/EVA decreased the PVC particle diameter from 0.5 to 0.05 µm (see Fig. 32). Hardt (6) claims that grafts with 80% EVA are completely compatible with PVC.

EVA-63. When EVA-45 is replaced by EVA-63, Shur and Rånby (38) have shown that the permeability of $O_2$ and $N_2$ in PVC/EVA blends changes markedly (see Fig. 33). First the signs of phase inversion at 4-7.5% EVA are less pronounced at 160°C and have diappeared at 180°C. Secondly the curve approached a straight line at 180°C, which is to be expected for a plasticized PVC. Other indications of increased compatibility were obtained from density measurements (see Fig.34) and DMS data (see Fig.35) The former showed a volume contraction and the latter a mobile EVA peak and a static PVC peak as the composition of the blend was changed. The DMS data could be interpreted in terms of an EVA rich phase containing dissolved or microdomains of PVC and a remaining PVC phase.

TEM studies (39) have clearly revealed the phase structure of PVC/EVA-63 blends, milled at 160 and 180°C (see Fig.36). The micrographs show that at 160°C EVA starts to form a network already at the content of 2%. At higher contents EVA seems to penetrate some of the smaller

Fig.27

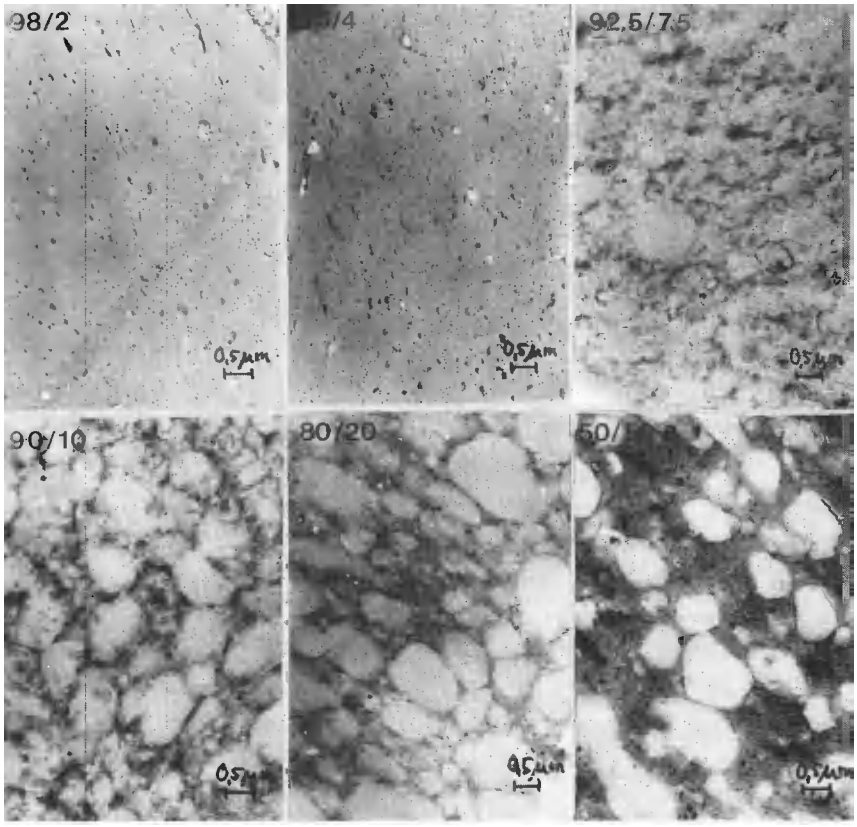


Fig.28

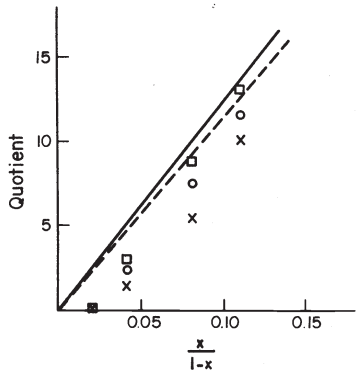


Fig.29

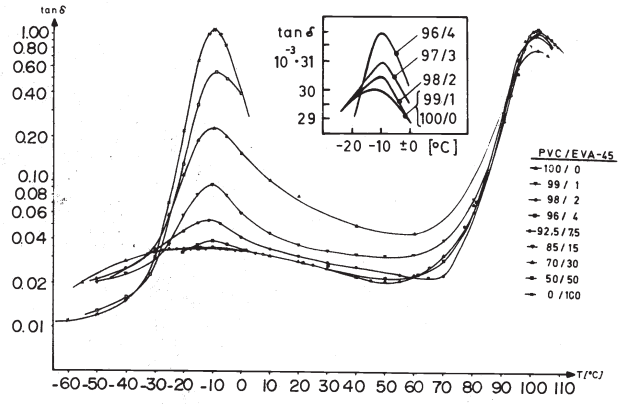


Fig.27. Transmission electron micrographs of PVC/EVA-45 blends showing phase inversion at 7.5 wt% EVA. EVA is stained by the $NaOH/Oso_4$ method; ref.(32).

Fig.28. Quotient between the intensities of the narrow (EVA phase) and the broad line (PVC phase) in the derivative NMR absorption spectra of blends. Full and dashed lines represent blends having the components completely separated in different phases: (X) blends milled at 160°C; (O) blends milled at 160°C and annealed 20 min. at 170°C; (□) blends milled at 160°C and annealed 40 min. at 170°C; ref.(34).

Fig.29. Mechanical loss tangent at 35 Hz vs. temperature for PVC/EVA-45 blends milled at 160°C; ref.(35).

Fig.30

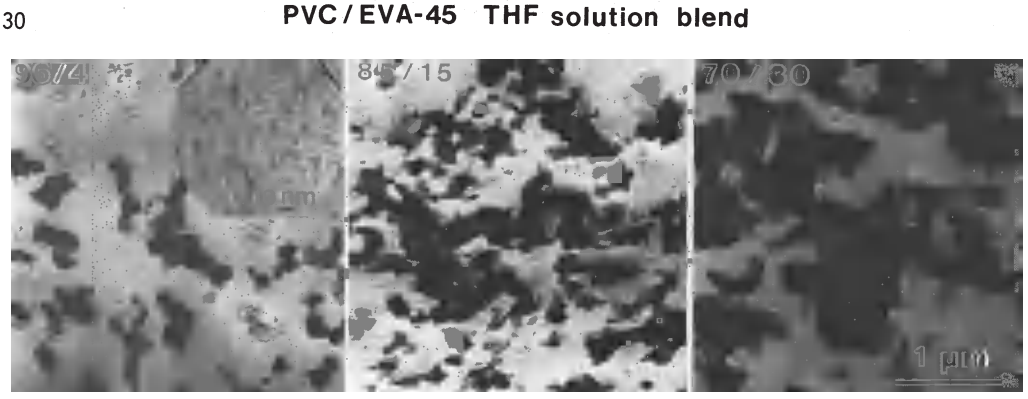


Fig.31

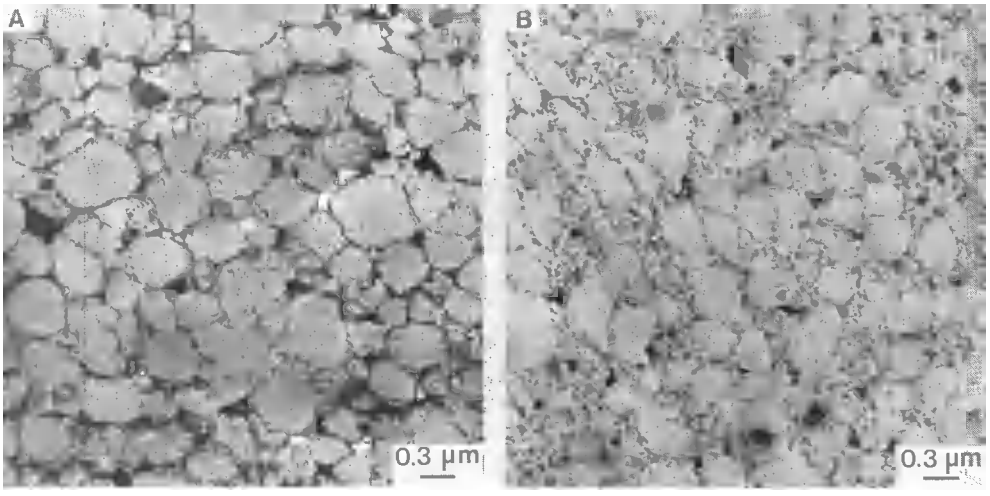


Fig.32

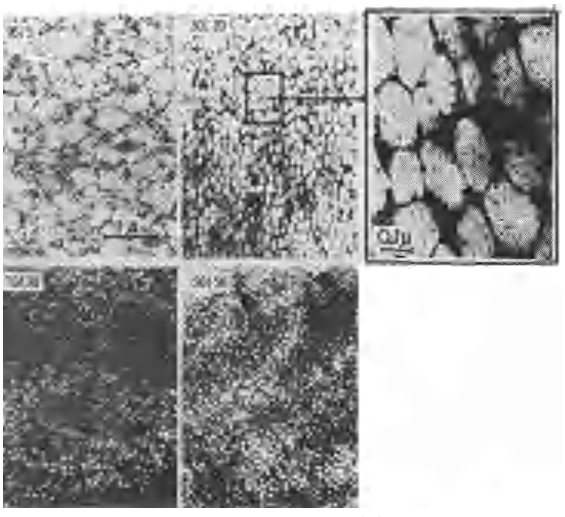

Fig.30. Transmission electron micrographs of THF solution blends of PVC/EVA-45 with inserted large magnification of $NaOH/OsO_4$-stained EVA phase showing EVA rich microdomains of 10 nm size; ref.(39).

Fig.31. Transmission electron micrographs of grafted PVC/EVA-45 (92.5/7.5) milled at 160°C (A) and 180°C (B); ref.(39).

Fig.32. Electron micrographs of PVC/EVA graft copolymers. EVA is stained by the $NaOH/OsO_4$ method; ref.(37).

Fig.33

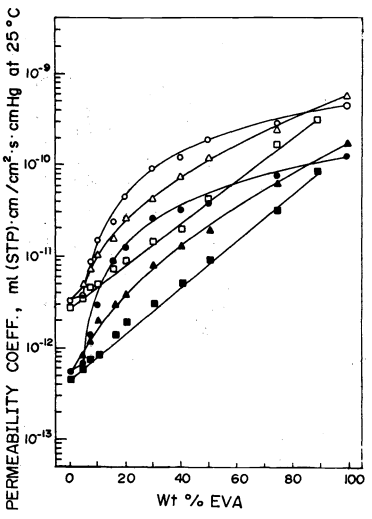


Fig.34

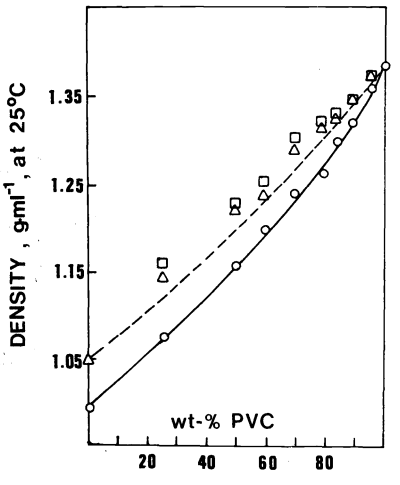


Fig.33. Permeability coefficients vs. blend composition in PVC/EVA blends (●○) PVC/EVA-45, milled at 160°C; (▲△) PVC/EVA-63 milled at 160°C; (■□) PVC/EVA-63, milled at 180°C. Open symbols denote oxygen, closed symbols denote nitrogen; ref.(38).

Fig.34. Experimental and calculated densities of the blends vs. blend composition: (○) PVC/EVA-45, milled at 160°C; (△) PVC/EVA-63, milled at 160°C; (□) PVC/EVA-63, milled at 180°C; ref.(38).

PVC particles and the surface layer of the larger ones. Thus the sensitivity of the EVA transition to blend composition (see Fig.36) can be explained by contamination of the EVA phase with fragments of disintegrated PVC-particles. At 180°C milling temperature an EVA network with micronsized mesh never seems to be established. Instead a network of the order of 0.05 µm mesh size is developed at 15 to 30% EVA enclosing subprimary PVC particles.

The tendency of EVA-63 to form a network already at 2% content can be explained by the low melt viscosity of EVA and the polarity match of PVC and EVA, factors that promote wetting of the PVC primary particle surface by EVA.

At higher processing temperature (180°C) the stability of the primary PVC particles is lost by interparticle segmental diffusion. However, the segmental compatibility of PVC and EVA prevents fusion of the particles and favours disintegration into microparticles surrounded by EVA.

Polyvinylacetate (PVA). Electron micrographs of nonstained PVC/PVA blends at 160°C (see Fig. 37, ref. 39) show PVA as dispersed domains of the order of 0.05 µm at 4% PVA and 0.5 µm at 7.5%. From 15%, PVA forms a continuous phase. For blends processed at 180°C the phase inversion occurs at 30% PVA.

At 160°C the lower melt viscosity of PVA has a lubricating and thus preserving effect on the PVC particles. At 180°C the fusion of PVC particles tends to disperse PVA and shift the inversion to higher PVA contents.

Solution blending seem to shift the inversion to still higher PVA contents (39,66).

Miscellaneous. Hammer (40) made torsional pendulum studies of PVC/EVA blended on roll mill at 190°C and in 10% THF solution. Two $T_g$:s were found at VA contents in EVA from 18 to 40% (EVA-45 was not included in the study), one $T_g$ at 65 and 70% and two $T_g$:s at 100% VA.

Probe Size for Characterization Methods. Feldman and Rusu (41) have reported one single glass transition for PVC/EVA-45 blends milled at 165°C based on dielectric loss measurements at 1 MHz. This raises the question of phase resolution limit or probe size of the characterization method.

Fig.35

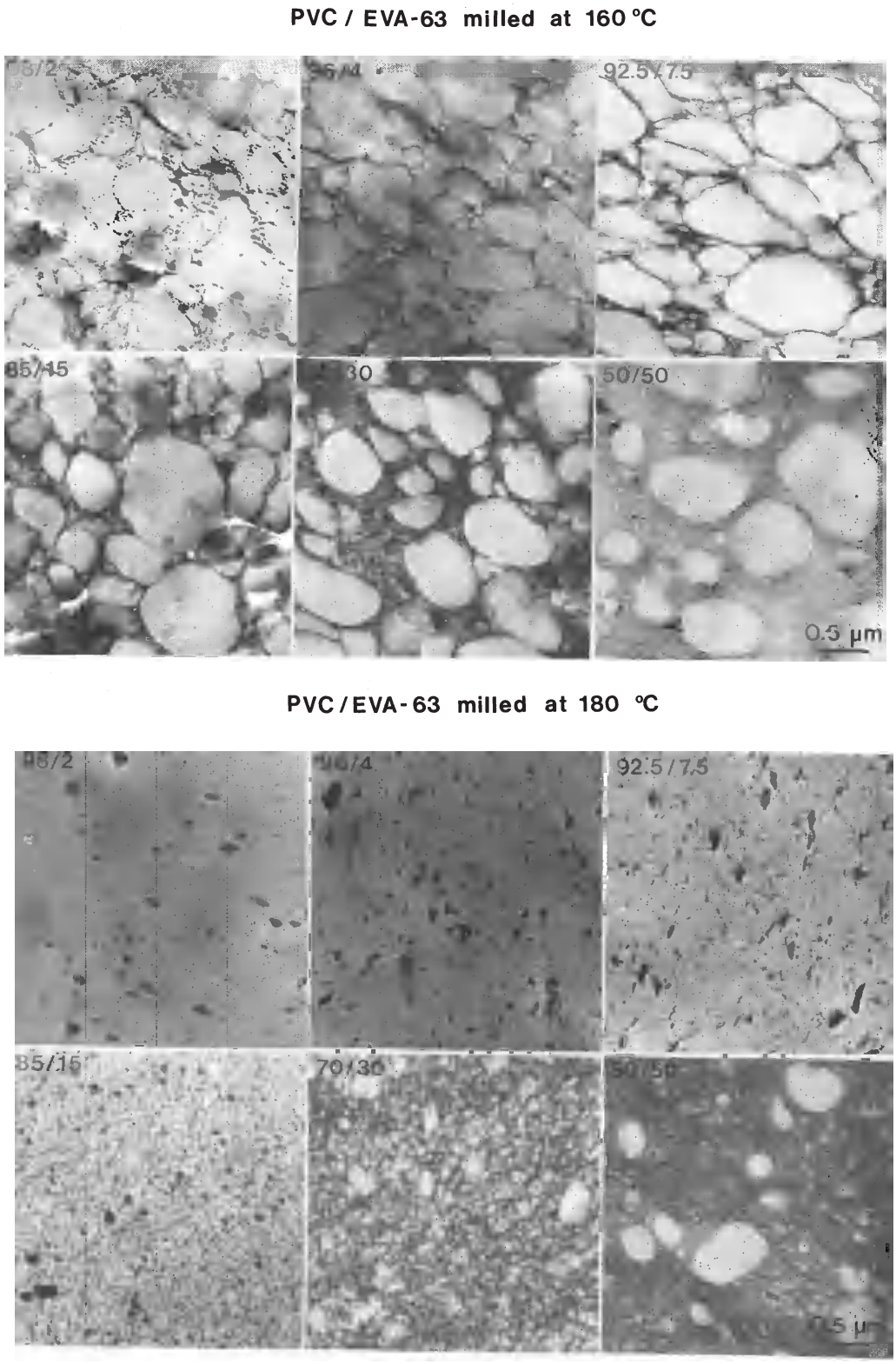


Fig.35. Electron micrographs of PVC/EVA-63 blends of different composition, milled at 160°C and 180°C; ref.(39).

Based on a review of several morphological studies Kaplan (42) concluded that the probe size of DMS was 15 nm or 100 to 5000 C-atoms. This is considerably more than the 10 to 30 C-atoms as proposed by Hammer (40). Stoelting et al (43) and others (44) have observed that DSC and dielectric measurements seem to be less sensitive to cooperative short range motions of segments than DMS.

Chlorinated Polyethylene (CPE)

Suspension chlorinated polyethylene (CPE) contains randomly distributed chlorine subtituted along the polyethylene chains. CPE can thus be considered as a terpolymer composed of ethylene, vinylchloride and 1,2 dichloroethylene segments (45). The presence of vinylidene units has also been suggested (46). The stiffness depends on crystallinity and polarity of CPE and the polarity increases with chlorine content (see Fig.38).

Fleischer and Brandrup (5,47,48) studied the effect of milling time and temperature on the rheology, morphology and properties of PVC blends with CPE of 30-40 wt% chlorine. Rheological measurements at 160°C (48) showed a stable low viscous melt flow evidently controlled by a continuous CPE phase embedding PVC primary particles. At 190°C the melt viscosity decreased rapidly with milling time indicating an inversion to PVC as continuous phase due to particle fusion. These findings were supported by turbidity measurements showing a strong opacity independent of milling time at 160°C but rapidly decreasing for increased milling time at 190°C. The shear modulus was found to decrease with increasing CPE up to 35% in agreement with calculated values according to Davies' interpenetrating network model (49) at 160°C and Nielsen's sphere-in-matrix model (50) at 190°C. The effect of processing was further evidenced by TEM. For this purpose a new staining technique for this system was developed (47). A strong base, the bicyclic amine diazobicyclo-undecene (DBU), was found to dehydrochlorinate CPE selectively at 0°C introducing osmiofilic double bonds in the CPE phase. Thus the network structure was confirmed at 10 wt% CPE, milled at 160°C (see Fig.39) while at 190°C the network was broken down to small dispersed particles.

Shur and Rånby (51) found indications of a phase inversion below 10% of CPE with 36, 42 and 48 wt% Cl respectively from gas permeability measurements with $O_2$, $N_2$ and $CO_2$ as penetrants.

DMS measurements (51) showed no peak shifts for blends with CPE-36 and 42 but a considerable shift of both peaks in PVC/CPE-48 blends. Similar results were reported by Locke and Paul

Fig.36

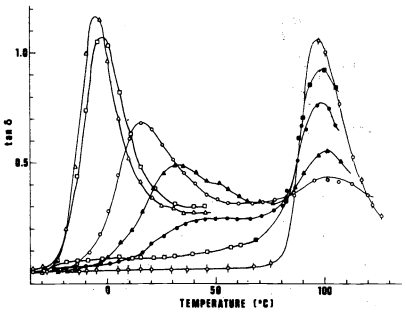


Fig.36. Mechanical loss tangent vs. temperature for PVC/EVA-63 blends, milled at 160°C; (△) 10/90, (□) 25/75, (0) 50/50, (▲) 70/30, (●) 85/15, (■) 92.5/7.5, (○) 100/0; ref.(38).

(52), Zelinger (53) and Work (54). Thus PVC blends with CPE containing 42% or less chlorine are incompatible and blends with CPE with 48% chlorine are semicompatible with PVC.

Influence of Process Parameters on Phase Structure.

Thus for blends of PVC with a rubbery homogenous amorphous polymer the phase structure seems to be controlled primarily by compatibility at mechanical blending and method of blending and processing temperature as indicated in Table 3.

TABLE 3.

| Process temperature | Rubber phase<br>Segmental compatibility with PVC | | |
|---|---|---|---|
| | bad<br>PBD,PVA | medium<br>NBR-20,CPE-36<br>EVA-45 | good<br>NBR-40,EVA-63 |
| Below critical temperature of fusion | inversion from dispersed to continuous phase at medium contents (≈15%) | inversion from fine dispersion to network at low contents (≈6-8%) | inversion from fine dispersion to network at very low contents (≈2%) |
| Above critical temperature of fusion | inversion from dispersed to continuous phase at high contents (≈30%) | inversion from fine disperse to continuous phase at medium contents (≈15%) | fine dispersion of microphases at all contents |
| Solution blend | inversion at ≈50% | inversion at ≈30% | fine dispersion at all contents |

Fig.37

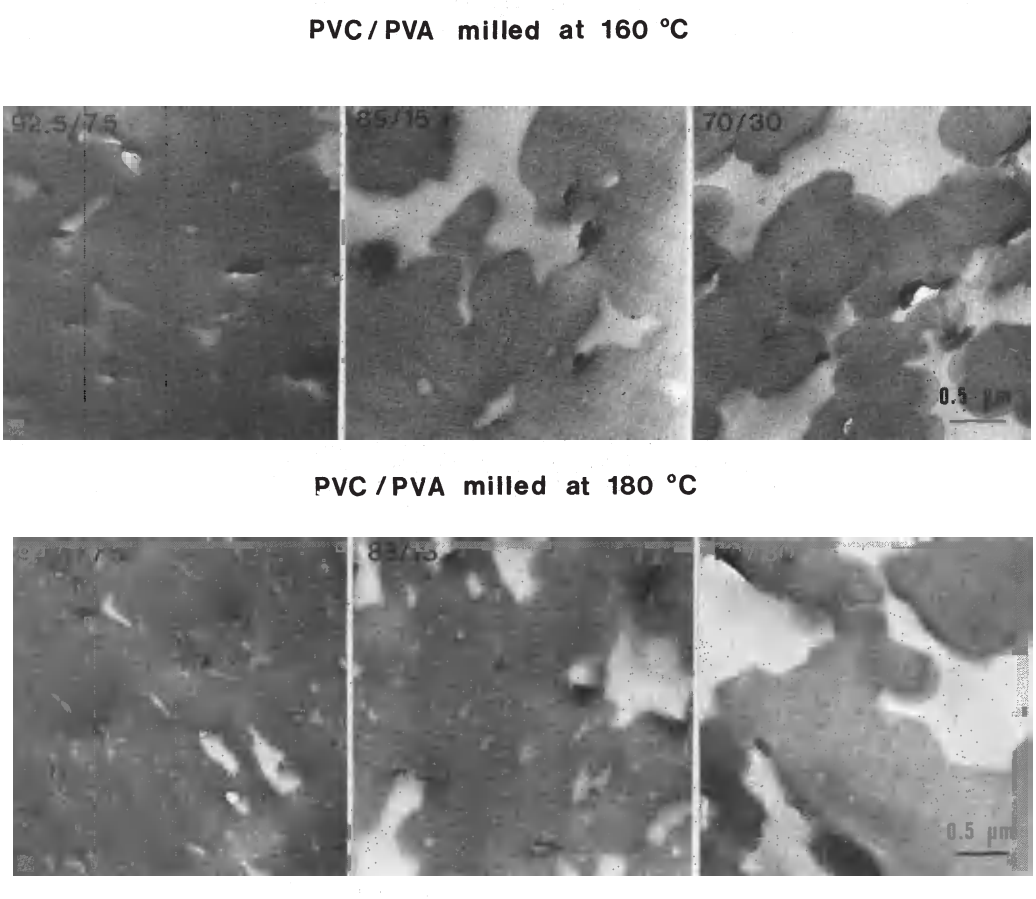


Fig.37. Electron micrographs of PVC/PVA blends of different composition, milled at 160 and 180°C; ref.(39).

Fig.38

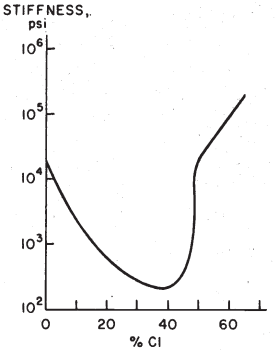


Fig.39

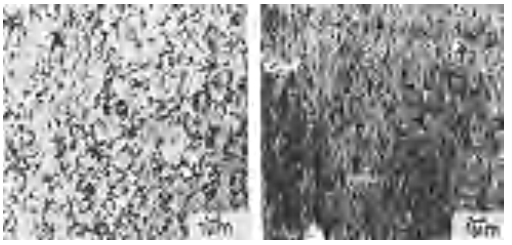

Fig.40

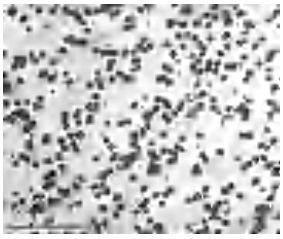

Fig.38. Stiffness vs. chlorine content of chlorinated polyethylene (CPE); ref.(67).

Fig.39. Electron micrographs of PVC/CPE (90/10) blends, processed at (A) 160°C and (B) 180°C; The CPE phase is stained by a DBU/$OsO_4$;ref.(5).

Fig.40. Electron micrograph of a PVC/MBS 100/10 blend showing even dispersion of rubber particles. The rubber phase is stained by $OsO_4$;ref.(15).

ABS, MBS and Acrylics.

So far we have dealt with homogenous (one phase) polymer modifiers for PVC. Thus NBR, EVA and CPE of suitable composition are capable of forming impact resistant network structures in PVC by moderate mechanical blending. However, heterogenous (two phase) graft copolymers like ABS and MBS are frequently used as modifiers for PVC. These contain grafted and crosslinked rubber particles of the order of 0.1 µm and are composed of butadiene homo- or copolymers. They are evenly dispersed in a hard matrix usually composed of a styrene copolymer with butadiene and acrylonitrile (ABS) or methylmethacrylate (MBS). By mechanical blending of these grafts with PVC the rubber particles are evenly dispersed in a homogenized matrix of PVC and the "hard" polymer of the graft modifier (1,8,15,39), see Fig.40. The impact strength of the blends is claimed to be insensitive to processing conditions (1).

Contrary to these findings Stabenow et al (55) and Fleischer and Brandrup (5) have reported network structures for PVC/MBS blends at moderate processing temperatures. Stabenow et al demonstrated a clear correlation between impact strength and network morphology. Milling for 10 min. at increasing temperatures was seen to increase the dispersion of rubber particles and the fusion of primary particles (see Fig.41). The same effect was obtained by increasing the degree of grafting and caused an impact strength reduction by a factor of five.

Grafting rubber with PVC may produce impact resistant network structures as with PVC-g-EVA-45 (92.5/7.5). On the other hand high impact PVC-grafts containing evenly dispersed rubber particles also exist. Röhrl (8) has described a PVC graft with crosslinked polyacrylate rubber particles forming a network structure on static heating but a fine and stable distribution of particles of the order of 0.1 µm at normal mechanical processing. The impact resistance was reported not to be dependent on processing conditions.

Fig.41

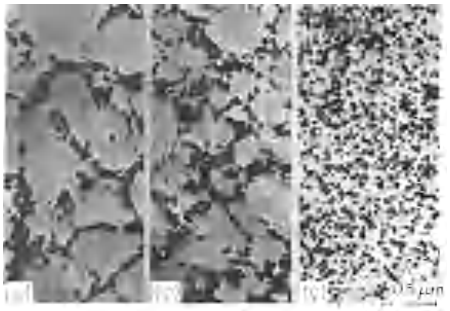

Fig.42

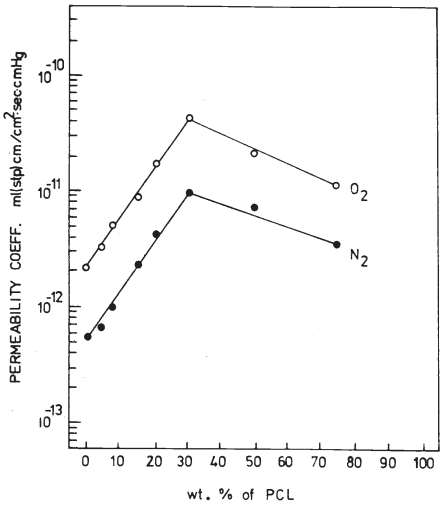


Fig.43

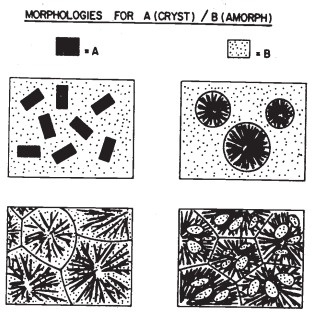


Fig.44

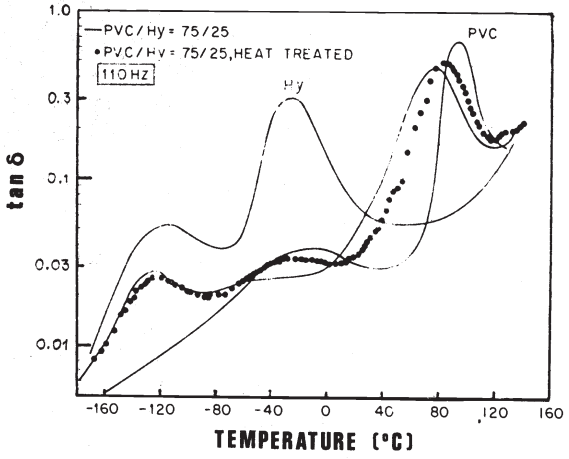


Fig.41. Electron micrographs of PVC blends with experimental MBS modifier of 25% grafting degree. The total amount of rubber in the blend was 6.7 wt%. The blend was milled at (A) 140°C, (B) 160°C, (C) 185°C; ref.(55).

Fig.42. Permeability coefficients vs blend composition for PVC/PCL blends. (○) $O_2$ (●) $N_2$; ref.(62).

Fig.43. Schematic illustration of possible morphologies of a binary blend having one crystallizable component; ref.(61).

Fig.44. Dynamic mechanical loss tangent at 110 Hz vs. temperature for PVC, Hytrel and PVC/Hytrel (75/25) blends; (●) annealed at 130°C; ref.(65).

Blends with a Crystallizable Polymer.

Polycaprolactone (PCL). PCL is a rather new commercial biodegradable polymer with a unique compatibility with other polymers. It has a crystallinity of about 50% and a melting point of 63°C.

At moderate concentrations PCL acts as a plasticizer for PVC forming transparent and flexible products. Koleske and Lundberg (56) found that these blends exhibit one single glass transition independent of blend composition when studied by DMS. By extrapolation from Gordon-

Taylor plots of $T_g$ for the blends the $T_g$ of PCL was estimated to -71°C. Above 30 wt% PCL, PVC is no longer able to prevent crystallization of PCL but only to decrease it. The partially crystalline blends become opaque and rigid as time elapses. The crystallization rate is increased at decreased content of PVC (57-61). Shur and Rånby (62) studied the gas transport properties of such blends and found no sign of phase inversion from log (permeability) - composition plots but a linear increase up to 30 wt% PCL followed by a linear decrease at higher contents of PCL (see Fig.42).

PCL rich blends with PVC were shown by polarized microscopy to be spherulitic. X-Ray microanalysis displayed a uniform distribution of chlorine in the spherulites (59,60). SAXS data were interpreted in terms of increasing lamellar spacing but invariant lamellar thickness with increased PVC content. This indicates a rejection of PVC to interlamellar regions of the spherulities (see Fig.43-C).

Low Contents of PCL. A reasonable consequence of the strong plasticizing effect of PCL on PVC at high PCL contents is an antiplasticizing effect at low contents of PCL. The presence of such an effect was also clearly demonstrated by Sundgren, Bergman and Shur (63). The following indications of antiplastication were found:

a) gradual suppression of the $\beta$-transition of PVC as measured by DMS and a shift of $\alpha$- and $\beta$-transitions to lower temperatures with increasing amount of PCL.

b) minimum of tensile creep compliance at about 6 wt-% PCL

c) maximum of stress limit of the linear viscoelasticity at 6 wt-% PCL

It is believed that ester groups of PCL form "pseudo-crosslinks" between PVC chains by strong polar interaction in a manner similar to the action of ester plasticizers like dioctyladipate (DOA) and dioctylsebacate (DOS). For complete suppression of the $\beta$-peak of plasticized PVC and for achieving maximum antiplastication effect (see b) and c) above) about twice as many ester groups per VC unit is required for PCL as for the fully compatible plasticizers DOA and DOS. Thus partial compatibility between PVC and PCL is suggested.

Copolyester (Hytrel). Hytrel$^R$ (du Pont) is composed of 70 wt-% of soft, amorphous tetramethyleneetherglycol terephtalate segments and 30 wt-% of hard, crystallizable tetramethylene terephtalate segments. By spin-lattice relaxation data at 30 MHz from pulsed NMR measurements and DMS data at 110 Hz on PVC/Hytrel blends, rapidly cooled from 150°C, Nishi and Kwei (64) have demonstrated the existence of one single glass transition at a temperature, shifting with blend composition. Thus extensive interaction between PVC and the soft segments of Hytrel is suggested. However, a significant amount of hard segments remains segregated as microcrystallites as evidenced by melting endoterms in DSC. Upon annealing at 130°C the soft segments are segregated from PVC and a miscibility gap associated with upper critical solution temperatures of 130-150°C is postulated. Annealing of 75/25 blends caused a phase separation that released the $\beta$-relaxation of PVC (see Fig.44). This explains the increase in impact strength observed at annealing (65).

The phase domains of heat treated samples was estimated to be as small as 10 nm from pulsed NMR data. This is due to the restrictions on phase separation imposed by the hard, crystalline segments of the Hytrel chains.

REFERENCES, part 1, PVC


1. Collins, E.A., Polymer Eng. Sci., 14 (5), 317 (1974).
2. Cotman, J.D., Ann. New York Acad. Sci., 57, 417 (1953).
3. Bier, G. and Kramer, H., Kunststoffe, 46 498 (1956).
4. Boccato, G., Rigo, A., Talamini, G. and Zilio-Grandi, F., Macromol. Chem., 108, 218 (1967).
5. Burnett, G.M., Ross, F.L. and Hay, J.N., J. Polymer Sci., A-1,5, 1467 (1967).
6. Nakajima, A., Hamada, H. and Hayashi, S. Macromol. Chem., 95, 40 (1966).
7. Schröder, E., Bühler, K., Franz, J. and Thinius, K., Plaste Kautchuk, 17, 629 (1970).
8. Rigo, A., Palma, G. and Talamini, G., Macromol. Chem., 153, 219 (1972).
9. Abbås, K.B., Bovey, F.A. and Schilling, F.C., Macromol. Chem. Suppl., 1, 227 (1975).
10. Bovey, F.A., Abbås, K.B., Schilling, F.C. and Starnes, W.H., Macromolecules, 8 437 (1975)
11. Baker, C., Maddams, W.F., Park, G.S. and Robertson, B., Macromol. Chem., 165, 321 (1973).
12. Abbås, K.B. and Sörvik, E.M., J. Appl. Polymer Sci., 19, 2991 (1975).
13. Abbås, K.B., J. Macromol. Sci.-Phys., B14 (1), 159 (1977).
14. Park, G., J. Macromol. Sci.-Phys., B14 (1), 159 (1977).
15. Brighton, C.A., Advances in PVC Compounding and Processing, MacLaren and Sons, London, 1962, p.1.
16. Trautvetter, W., Macromol. Chem., 101, 214 (1967).
17. Natta, G. and Corradini, J., J. Polym. Sci., 20, 251 (1956).

18. Talamini, G. and Vidotto, G., Macromol. Chem., 100, 48 (1967).
19. Bovey, F.A., Hood, F.R., Anderson, E.W. and Kornegay, R.L., J. Phys. Chem., 71, 312 (1967).
20. Cavalli, L. and Carraro, G., Illinois Institute of Technology, NMR, Newsletter No. 110 (nov. 1967).
21. Germar, H., Hellwege, K.H. and Johnsen, U., Macromol. Chem., 60, 106 (1963).
22. Pezzin, G., Plastics and Polymers, 37, 295 (1969).
23. Abdel-Alim, A.H. and Hamielec, A.E., J. Appl. Polymer Sci., 17, 3033 (1973).
24. Leaderman, H., Ind. Eng. Chem., Prod. Res. Dev., 35, (3), 374 (1943).
25. Alfrey, T., Weiderhorn, N., Stein, R., Tobolsky, A., J. Colloid Sci., 4, 211 (1949).
26. Pezzin, G., J. Macromol. Sci.-Phys. B14 (2), 323 (1977).
27. Münstedt, H., J. Macromol. Sci.-Phys., B14 (2), 195 (1977).
28. Wilkes, C.E., Folt, V.L. and Krimm, S., Macromol., 6 (2), 235 (1973).
29. Lebedev, V.P., Okladov, N.A., Minsker, K.S. and Schtarkman, B.P., Vysokomol. Soyed., 7, 655 (1965).
30. Glazkovskii, Y.V., Zgayevskii, V.E., Ruchninskii, S.P. and Bakardzhiyev, N.M., Vysokomol, Soyed., 8, 1472 (1966).
31. Garbuglio, G., Rodella, A., Borsini, G.C. and Gallinella, E., Chim. Ind. (Milan), 46, 166 (1964).
32. Manson, J.A., Iobst, S.A. and Acosta, R.A., Polymer Preprints, 13 (2), 1175 (1972).
33. Wenig, W., J. Polymer Sci., Polymer Phys. Ed., 16, 1635 (1978).
34. Nielson, G. and Jabarin, S., J. Appl. Phys., 46, 1175 (1975).
35. Rehage, G. and Halboth, H., Macromol. Chem. 119, 235 (1968).
36. D'Amato, R.J. and Strella, S., Appl. Polymer Symp., 8, 275 (1969).
37. Singleton, C., Isner, J., Gesovitch, D.M., Tsou, P.K.C., Geil, P.H. and Collins, E.A., Polym. Eng. Sci., 14 (5), 371 (1974).
38. Straff, R.S. and Uhlmann, D.R., J. Polymer Sci., Polymer Phys. Ed., 14, 353 (1976).
39. Ohta, S., Kajiyama, T. and Takanayagi, M., Polym. Eng. Sci., 16, 465 (1976).
40. Wilski, H., Kolloid Zeit., 210, 37 (1966).
41. Prietzschk, A., Kolloid Zeit., 156, 8 (1958).
42. Juijn, J.A., Gisolf, J.H. and de Jong, W.A., Kolloid Zeit., 251, 456 (1973).
43. Stokr, J., Scheider, B., Kolinsky, M., Ryska, M. and Lim, D., Intern. Symp. Makrom. Chem, Tokyo, 1966,
44. Hellwege, K.H., Johnsen, U. and Kockott, D., Kolloid Zeit., 194, 5 (1964).
45. Pohl, K.U. and Hummel, D.O., Macromol. Chem., 113, 203 (1968).
46. Kockott, D., Kolloid Zeit., 198, 17 (1964).
47. C.f. W.J. Frissell, Encyclopedia of PVC (L.I. Nass, Ed.) Chapt. 7. Elucidation of structure (p. 263). Marcel Dekker, New York, 1976.
48. Barclay, M., Angew. Macromol. Chem., 52, 1 (1976).
49. Shinagava, Y. Plast. Ind. News, p. 65 (1973).
50. Cotman, J.D., Gonzales, M.F. and Claver, G.C., J. Polymer Sci., A-1 5, 1137 (1967).
51. Tregan, R. and Bonnemayre, A., Plast. Mod. Elast. 23, 220 (1971).
52. Bort, D.N., Marinin, V.G., Kalinin, A.I. and Kargin V.A., Vysokomol, Soyedin., A, 10, 2574 (1968).
53. Behrens, H., Plaste Kaut., 22, 2 (1975).
54. Palma, G., Talamini, G., Tavan, M. and Carenza, M., J. Polymer Sci., Polymer Phys. Ed., 15, 1537 (1977).
55. Mickley, H.S., Michaels, A.S. and Moore, A.L., J. Polymer Sci., 60, 121 (1962).
56. Davidson, J.A. and Whitenhafer, Abstract paper at ACS conf., 1979, p. 94.
57. Hattori, T., Tanaka, K. and Matsuo, M., Polymer Eng. Sci., 12 (3 ), 203 (1972).
58. Rootare, H.M. and Nyce, A.C., Int. J. Powder Met., 7, 3 (1971).
59. Krzewki, R.J. and Sieglaff, C.L., Polymer Eng. Sci., 18 (15), 1174 (1978).
60. Geil, P.H., J. Macromol. Sci.- Chem., A11 (7), 1271 (1977).
61. Mooney, M. and Wolstenholme,W.E., J. Appl. Phys., 25, 1098 (1954).
62. Berens, A.R. and Folt, V.L., Trans. Soc. Rheol., 11 (1), 95 (1967).
63. Collins, E.A., Pure Appl. Chem., 49, 581 (1977).
64. Collins, E.A. and Krier, C.A., Trans Soc. Rheol., 11 (2) 225 (1967).
65. Collins, E.A. and Metzger, A.P., Polymer Eng. Sci., 10, 57 (1970).
66. Berens, A.R. and Folt, V.L., Polymer Eng. Sci., 9 (1), 27 (1969).
67. den Otter, J.L., Wales, J.L.S., Schwarzl, F.R., Proc. International Congress on Rheol., Lyon (1972).
68. Khanna, R., S.P.E.J., 29, 48 (1973).
69. Münstedt, H., Angew. Macromol. Chem., 47, 229 (1975).
70. Menges, G. and Berndtsen, N., Pure Appl. Chem., 49, 597 (1977).
71. Berndtsen, N., Dissert. Inst. Kunststoffverarbeitung, Aachen.
72. Faulkner, P.G., J. Macromol. Sci.-Phys., B11 (2), 251 (1975).
73. Bair, H.E., Matsuo, M., Salmon, W.A. and Kwei, T.K., Macromolecules, 5 (2), 114 (1972).
74. Bonart, R., Kolloid Zeit., 213 (1956).
75. Cobbold, A.J. and Mendelson, A.E., Science Tools, 18 (1), 1 (1971).
76. Hori, Y., Japan Plast., 3 (2), 48 (1969).

REFERENCES part 2, polymer blends


1. c.f. Ryan, C.F. and Jalbert, R.L., Encyclopedia of PVC (L.I.Nass ed.), Chapt. 12 (p. 602--642) Modifying resins for polyvinylchloride, Marcel Dekker, New York 1976.
2. Merz, E.H., Claver, G.C. and Baer, M., J. Polymer Sci., 22, 325 (1956).
3. Trautvetter, W., Macromol. Chem., 101, 214 (1967).
4. Matsuo, M., Ueda, A. and Kondo, Y., Polymer Eng. Sci., 10 (5), 253 (1970).
5. Fleicher, D., Scherer, H. and Brandrup, J., Angew. Macromol. Chem., 58/59, 121 (1977).
6. Hardt, D., Br. Polymer J., 1, 225 (1969).
7. Menzel, G., Hundertmark, G. and Polte, A., Kunststoffe, 67, 339 (1977).
8. Röhrl, E., Kunststoffe, 70, 41 (1980).
9. Nielsen, L., J. Amer. Chem. Soc., 75, 1435 (1953).
10. Schmeider, K. and Wolf, K., Kolloid Zeit., 134, 149 (1953).
11. Breuers, W., Hild, W. and Wolff, H., Plaste Kaut., 1, 170 (1954).
12. Takayanagi, M., Harima, H. and Iwatu, Y., Mem. Fac. Eng. Kyushu Imp. Univ., 23, 1 (1963).
13. Bohn, L., Kolloid Zeit., 213, 55 (1966).
14. Horwath, J., Wilson, W., Lundstrom, H. and Purdun, J., Appl. Polymer Symp. 7, 95 (1968).
15. Matsuo, M., Nozaki, C. and Jyo, Y., Polymer Eng. Sci., 9 (3), 197 (1969).
16. Shur, Y.J. and Rånby, B., J. Appl. Polymer Sci., 19, 2143 (1975).
17. Kato, K., Polymer Letter, 4, 35 (1966).
18. Landi, V.R., Appl. Polymer Symp., 25, 223 (1974).
19. Chandler, L. and Collins, E.A., J. Appl. Polymer Sci., 13, 1585 (1969).
20. Landi, V.R., Rubber Chem. Technol., 45, 222 (1972).
21. Jorgensen, A., Chandler, L. and Collins, E.A., Rubber Chem. Technol., 46, 1087 (1973).
22. Zakrzewski, G.A., Polymer, 14, 347 (1973).
23. Aiken, W.T., Alfrey, T., Janssen, A. and Mark, H., J. Polymer Sci., 2, 178 (1947).
24. Alfrey, T., Wiederhorn, N., Stein, R.S. and Tobolsky, A.V., J. Colloid Sci., 4, 211 (1949).
25. Sabia, A. and Eirich, F., J. Polymer Sci., A1, 2947 (1963).
26. Walter, A.T., J. Polymer Sci., 13, 207 (1954).
27. Bergman, G., Bertilsson, H. and Shur, Y.J., J. Appl. Polymer Sci., 21, 293 (1977).
28. Bertilsson, H. and Jansson, J.F., J. Appl.Polymer Sci., 19, 1971 (1975).
29. Storström, H., Tekn. L. thesis. Royal Institute of Technology, Stockholm, 1969.
30. Storström, H. and Rånby, B., Advan. Chem. Ser., 99, 107 (1971).
31. Terselius, B. and Rånby, B., Paper presented at IUPAC Int. Symp. Macromolecules, Leiden, September 1970, preprints of papers p. 559.
32. Terselius, B., Tekn. L. thesis, Royal Institute of Technology, Stockholm 1970.
33. Matsuo, M., private communication.
34. Elmqvist, C., Svanson, S.E., Shur, Y.J. and Rånby, B., J. Appl. Polymer Sci., 21, 943 (1977).
35. Gedde, U., M. Sc. thesis, Royal Institute of Technology, Stockholm, 1976.
36. Marcincin, K., Romanov, A. and Pollak, V., J. Appl. Polymer Sci., 16, 2239 (1972).
37. Jyo, Y., Nozaki, C. and Matsuo, M., Macromolecules, 4, 517 (1971).
38. Shur, Y.J. and Rånby, B., J. Appl. Polymer Sci., 19, 1337 (1975).
39. Terselius, B., unpublished data.
40. Hammer, C.F., Macromolecules, 4, 69 (1971).
41. Feldman, D. and Rusu, M., Europ. Polymer J., 10, 41 (1974).
42. Kaplan, D.S., J. Appl. Polymer Sci., 20, 2615(1976).
43. Stoelting, J., Karasz, F.E. and MacKnight, W.J., Polymer Eng. Sci., 10 (3), 133 (1970).
44. CF. W.J. MacKnight, F.E. Karasz and J.R. Fried, in Polymer Blends (eds. D.R. Paul and S. Newman), Chapt. 5 (p. 185-242), Academic Press, New York, 1978.
45. Oswald, H.J. and Kubu, E.T., SPE Transac, July 1963, p. 68.
46. Kalfoglou, N.K. and Williams, H.L.,Polymer Eng. Sci., 12 (3), 235 (1972).
47. Fleischer, D., Fischer, E. and Brandrup, J., J. Macromol. Sci.-Phys., B14 (1), 17 (1977).
48. Fleischer, D., Kloos, F. and Brandrup, J., Angew. Macromol. Chem., 62, 69 (1977).
49. Davies, W.E.A., J. Phys. D., 4, 318 (1971).
50. Nielsen, L.E., Rheol. Acta, 13, 86 (1974).
51. Shur, Y.J. and Rånby, B., J. Appl. Polymer Sci., 20, 3105 (1976).
52. Locke, C.E. and Paul, D.R., Polymer Eng. Sci., 13 308 (1973).
53. Zelinger, J., J. Polymer Sci. C., 16, 4259 (1969).
54. Work, J.L., Polymer Eng. Sci., 13 46 (1973).
55. Breuer, H., Haaf, F. and Stabenow, J., J. Macromol. Sci.-Phys., B14 (3), 387 (1977).
56. Koleske, J.V. and Lundberg, R.D., J. Polymer Sci., A-2, 7, 795 (1969).
57. Ong, C.J. Ph.D., thesis, University of Massachusetts, Armhurst, Mass., 1974
58. Ong.,C.J. and Price, F.P., J. Polymer Sci., Symp. Ser., 63 45 (1978).
59. Khambatta, F.B., thesis, University of Massachusetts, Armhurst, Mass., 1976.
60. Khambatta, F.B., Russel, T., Warner, F., and Stein, R.S., J. Polymer Sci., Polymer Phys. Ed., 14, 139 (1976).
61. Stein, R.S., Khambatta, F.B., Warner, F.P., Russel, T., Escala, A and Balizer, E., J. Polymer Sci., Symp. Ser., 63, 313 (1978).
62. Shur, Y.J. and Rånby, B., J. Macromol. Sci.-Phys., B14 (4), 565 (1977).
63. Sundgren, N., Bergman, G. and Shur, Y.J., J. Appl. Polymer Sci., 22, 1255 (1978).

64. Nishi, T., Kwei, T.K. and Wang, T.T., J. Appl. Phys., 46 (10), 4157 (1975).
65. Nishi, T. and Kwei, T.K., J. Appl. Polymer Sci., 20, 1331 (1976).
66. Schneider, I.A. and Vasile, C., Europ. Polymer J., 6, 684 (1970).
67. C.f. G.D. Jones, Chemical reactions of polymers (E.M. Fettes ed.), Chapt. 3 (p. 247), Wiley, New York 1964.